PNAS

Proceedings of the National Academy of Sciences
of the United States of America
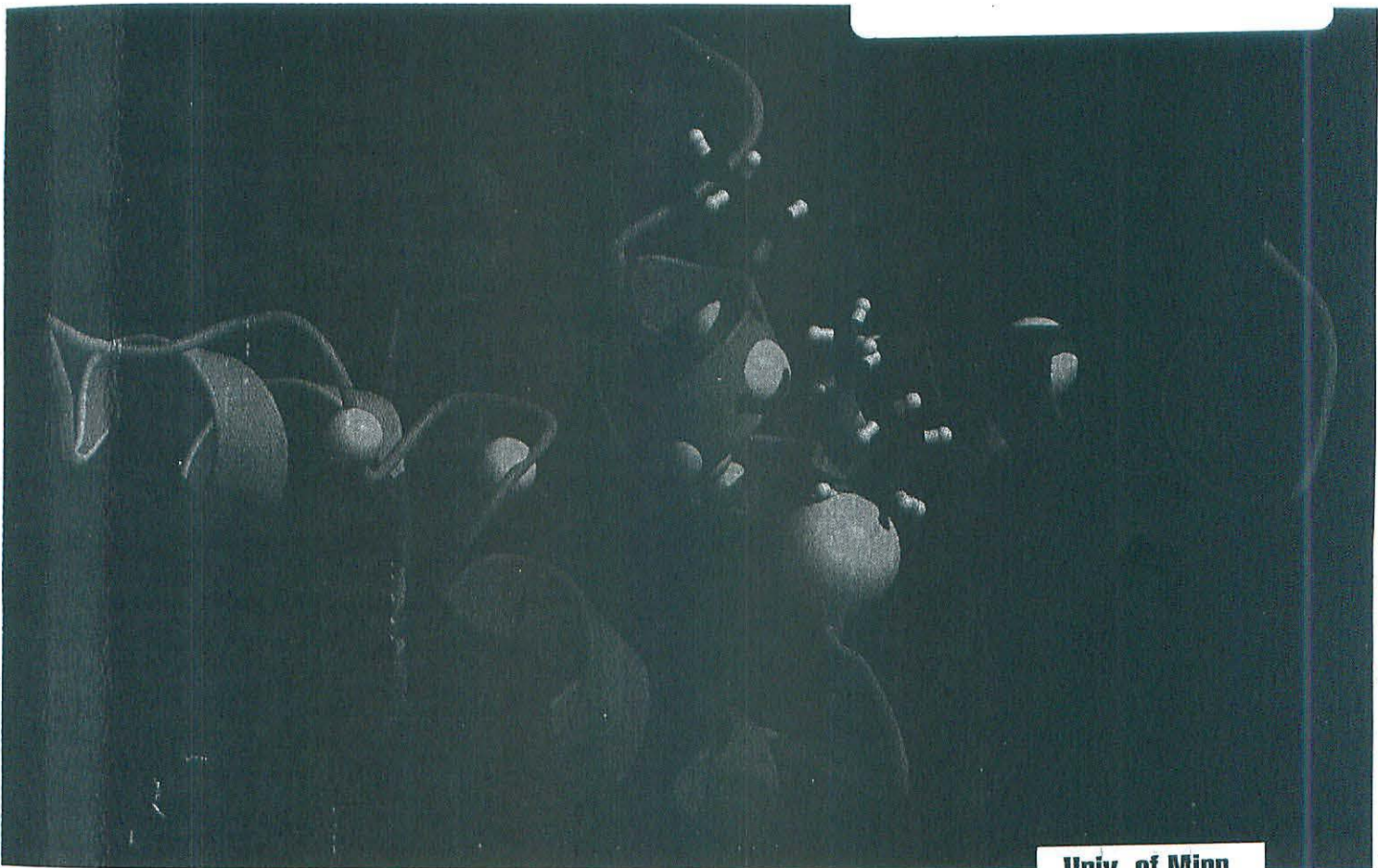
Where the poly(A)-binding protein binds translation factors

Ancient carbon cycle tells of past biological diversity

New World patterns of human migration

Retrovirus linked with schizophrenia

Pharmaceutical intervention for weight control

PTEN controls tumor-induced angiogenesis

Shenghua Wen*, Javor Stolarov†, Michael P. Myers†, Jing Dong Su*, Michael H. Wigler†, Nicholas K. Tonks†, and Donald L. Durden*‡

*Section of Hematology/Oncology, Department of Pediatrics, Herman B Wells Center for Pediatric Research, Department of Biochemistry and Molecular Biology, Indiana School of Medicine, Indianapolis, IN 46202; and †Cold Spring Harbor Laboratory, Cold Spring Harbor, NY 11724

Mutations of the tumor suppressor PTEN, a phosphatase with specificity for 3-phosphorylated inositol phospholipids, accompany progression of brain tumors from benign to the most malignant forms. Tumor progression, particularly in aggressive and malignant tumors, is associated with the induction of angiogenesis, a process termed the angiogenic switch. Therefore, we tested whether PTEN regulates tumor progression by modulating angiogenesis. U87MG glioma cells stably reconstituted with PTEN cDNA were tested for growth in a nude mouse orthotopic brain tumor model. We observed that the reconstitution of wild-type PTEN had no effect on *in vitro* proliferation but dramatically decreased tumor growth *in vivo* and prolonged survival in mice implanted intracranially with these tumor cells. PTEN reconstitution diminished phosphorylation of AKT within the PTEN-reconstituted tumor, induced thrombospondin 1 expression, and suppressed angiogenic activity. These effects were not observed in tumors reconstituted with a lipid phosphatase inactive G129E mutant of PTEN, a result that provides evidence that the lipid phosphatase activity of PTEN regulates the angiogenic response *in vivo*. These data provide evidence that PTEN regulates tumor-induced angiogenesis and the progression of gliomas to a malignant phenotype via the regulation of phosphoinositide-dependent signals.

The reversible phosphorylation of proteins and lipids is critical to the control of signal transduction in mammalian cells and is regulated by kinases and phosphatases (1). The product of the tumor suppressor gene PTEN/MMAC (hereafter termed PTEN) was identified as a dual specificity phosphatase and has been shown to dephosphorylate inositol phospholipids (2–9). The PTEN gene is mutated in 40–50% of high-grade gliomas as well as prostate, endometrial, breast, lung, and other tumors (2, 3, 10). In addition, PTEN is mutated in several rare autosomal dominant cancer predisposition syndromes, including Cowden disease, Lhermitte-Duclos disease, and Bannayan-Zonana syndrome (11–14). The phenotype of PTEN-knockout mice reveal a requirement for this phosphatase in normal development and confirm its role as a tumor suppressor (15–17).

PTEN is a 55-kDa protein comprising an N-terminal catalytic domain, identified as a segment with homology to the cytoskeletal protein tensin and containing the sequence $HC(X)_5R$, which is the signature motif of members of the protein tyrosine phosphatase family, and a C-terminal C2 domain with lipid-binding and membrane-targeting functions (18). The sequence of the extreme C terminus of PTEN suggests a function in binding PDZ domain-containing proteins. PTEN is a dual specificity phosphatase that displays a pronounced preference for acidic substrates (5). Importantly, PTEN possesses lipid phosphatase activity, preferentially dephosphorylating phosphoinositides at the D3 position of the inositol ring. It is the only enzyme known to dephosphorylate the D3 position in inositol phospholipids, suggesting that PTEN may function as a direct antagonist of phosphatidylinositol 3-kinase (PI3-kinase) and phosphatidylinositol 3,4,5-trisphosphate [$PtdIns(3,4,5)P_3$]-dependent signaling (7, 13). Reconstitution of PTEN in tumor cells that carry mutations in the PTEN gene have established that this phosphatase regulates the PI3-kinase-dependent activation of AKT, a major player in cell survival (6, 14). However, despite progress in understanding the biochemistry of PTEN,

the role of this phosphatase in tumor progression, as it relates to its diverse effects on cell growth, angiogenesis, and/or survival, remains unclear.

Mutations in PTEN accompany progression of brain tumors from grade I/II to malignant grade III and IV *in vivo* (19, 20). Tumor progression is associated with angiogenesis, the formation of new blood vessels from existing vascular structures, with increases in microvessel density (MVD) and increased invasion of tumor cells into brain parenchyma (21–23). For tumor growth to occur, tumor dormancy must be broken, an event termed the angiogenic switch. During angiogenesis endothelial cells are induced to degrade the basement membrane of existing vessels, break away, and migrate to the site of the tumor, where they proliferate to form linear structures that differentiate to form blood vessels. Factors that control angiogenesis include growth factors, matrix metalloproteinases, plasminogen activators, thrombospondins, integrins $\alpha v \beta 3$, $\alpha v \beta 5$, and $\alpha 5 \beta 1$, etc. (23–25). The angiogenic switch involves a shift in the balance of angiogenic stimulators and angiogenic inhibitors. Stimulators include the growth factors, vascular endothelial growth factor and basic fibroblast growth factor, and the induction of matrix remodeling via matrix metalloproteinases (26). Inhibitors include thrombospondin 1 (TSP-1), angiostatin, endostatin, tissue inhibitors of metalloproteinases, and others (24, 27). It has been observed that neovascularization and PTEN mutations are associated with high-grade gliomas and are not observed in low-grade glial tumors, leading to the hypothesis that these two events may be causally linked.

Regulation of PI3-kinase-dependent signals, including activation of AKT by vascular endothelial growth factor and its receptors, the protein tyrosine kinases Flt-1 and KDR, have been implicated in brain tumor angiogenesis (28). Data generated in the chicken chorioallantoic membrane model suggests that PI3-kinase-dependent pathways may regulate angiogenesis and vascular endothelial growth factor expression in endothelial cells (29). Furthermore, correlative studies in prostate tumor specimens have demonstrated that tumors containing PTEN mutations have higher microvessel counts than tumors expressing wild-type (WT) PTEN (30). However, whether PTEN is causally linked to induction of angiogenesis by the tumor cell remains unproven. These and other observations led us to hypothesize that PTEN may control tumor-induced angiogenesis and contribute to the high mortality associated with malignant brain tumors.

Materials and Methods

Cell Culture, Constructs, and Reagents. WT PTEN or mutant PTEN (G129E, R130 M) cDNAs were subcloned into the pBabe-puro retroviral expression vector. Stable clones of U87MG cells expressing WT PTEN (WT.E1, WT.C7) or mutant PTEN (G129E, R130 M) were established under puromycin selection

---

(2 μg/ml) (6). Muristirone-induced expression of PTEN in U87MG cells was performed as described by J. Stolarov (31). Antibodies were obtained specific for PTEN (6), AKT and phospho-S473-AKT (New England Biolabs, #9270), TSP-1 (Calbiochem, #605230), and anti-BrdUrd mAb clone BU33 (Sigma, #B9285).

Tumor Implantation. Cells were cultured in fresh medium for 24 h and harvested, adjusting the cell concentration to 1×10^6 in 10 μl of RPMI medium. Mice, under general anesthesia were placed into the stereotactic device (model 963, Kopf Instruments, Tujunga, CA). Stereotactically controlled drill assembly was used to provide a hole 0.3 mm deep and of 0.8 mm diameter in cranium at a position 0.5 mm anterior and 1.2 mm lateral to the bregmal anatomical landmark. Tumor cells (1×10^6) were introduced slowly through a 10-μl Hamilton syringe at a depth of 2.5 mm at a rate of 2 μl/min. We then slowly removed the needle at a rate of 0.5 mm/min. After needle removal we sealed the hole with bone wax and closed the incision with a wound clip. In some of the mice, 5×10^6 tumor cells were implanted s.c. into the right flank to monitor tumor volume and to perform biochemical and immunohistochemical analysis of tumor tissue. All animal experiments performed were approved by the Animal Care Committee at Indiana University School of Medicine.

Biochemical Analysis. Immunoblots were performed on cell lysates obtained from U87 cells grown in tissue culture or from multiple cryostat sections of s.c. tumor tissues. A Bradford assay was performed to determine protein concentration of each lysate. Equivalent amounts of protein were resolved by SDS/PAGE and transferred to nitrocellulose. Membranes were probed with antisera specific for PTEN, AKT, phospho-S473-AKT, or TSP-1. The RNase protection assay was performed by using a RPA III kit from (Ambion) according to the manufacturer's specifications. Briefly, 20 μg of total RNA was precipitated and resuspended in 10 μl of hybridization buffer containing the radioactive probe. The RNA then was heated to 95°C for 10 min and hybridized for 16 h at 42°C. A total of 150 μl of this mixture was treated with 1:100 dilution of RNase in RNase buffer for 30 min. RNase was inactivated, and RNA was reprecipitated and resolved on 5% acrylamide gel. RNA probes were synthesized by using MAXI SCRIPT using PCR templates and T7 polymerase. The glyceraldehyde-3-phosphate dehydrogenase probe was provided in the kit, and TSP-1 probe represents a 590-nt sequence in the 3′ untranslated region of TSP-1 sequence. All probes were sequenced.

Immunohistochemical Analysis. MVD was determined for each s.c. and brain tumors by CD31 staining, and a proliferative index was determined by using anti-BrdUrd mAb staining performed on cryostat sections (7 μm), fixed in acetone, blocked in 1% goat serum, and stained with anti-CD31 antibody (PharMingen, #01951D). Antibody staining was visualized with peroxidase-conjugated anti-mouse and counterstained with hematoxylin. A negative control was performed on each tumor tissue stained with mouse IgG. Two sections from each tumor were scanned under low-power magnification (×40) to identify areas of highest CD31-positive vessel density (32), followed by digitization of three fields from this area. For in vivo BrdUrd labeling, mice received 100 μl of BrdUrd in PBS (10 mM) injected into the tail vein 1 h before tumor harvesting. The digitized images representing one ×20 field were counted for the number of CD31-positive vascular elements and number of BrdUrd-positive cells/field. The number of cells positive for BrdUrd staining ranged between 5% and 8% of total number of tumor cells. Data were collected from two independent observers without knowledge of which tumors were viewed. The average number of microvessels or cells positive for BrdUrd staining per digitized field was
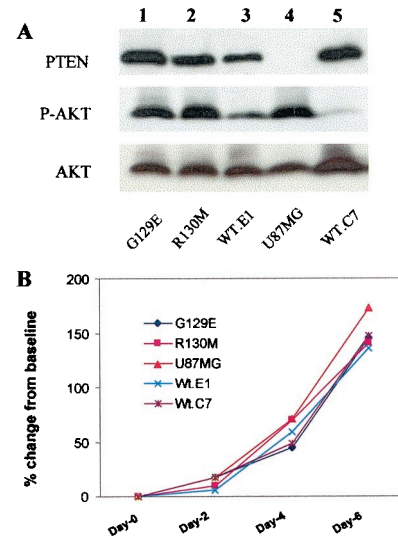

Fig. 1. Stable expression of PTEN and PTEN mutants in U87MG cells regulates AKT. (*A*) Cell lysates from the U87MG (U87) cell line and U87 cells infected with a retroviral vector encoding PTEN (pBabe-Puro-PTEN) or mutants of PTEN (pBabe-Puro-PTEN-G129E or R130 M) were resolved by SDS/PAGE, and equal amounts of proteins were loaded per lane, immunoblotted with antisera to PTEN, phospho-AKT, and total AKT, and visualized by enhanced chemiluminescence. The basal levels of PTEN (*Top*), phosphorylated AKT (Ser-473) (*Middle*), and total AKT (*Bottom*) are shown. The status of the PTEN gene in each stable cell line was designated as: WT.E1 and WT.C7, two separate clones expressing WT PTEN; R130 M and G129E are mutated PTEN, R130 M is inert as both a protein and a lipid phosphatase. The G129E PTEN can dephosphorylate acidic phosphopeptides, but cannot dephosphorylate lipid substrate, PtdIns(3,4,5)P$_3$. The U87MG (U87) cell line is the parental cell line isolated from a human glioblastoma multiforme patient. (*B*) Comparison of in vitro growth of U87MG cells transduced with mutants of PTEN. Equal number of cells (1×10^5) were incubated in RPMI + 10% FBS for different times, and cell numbers were quantitated by direct cell counting.

determined for five tumors per experimental group and analyzed by Student's *t* test.

Results

Effect of PTEN Reconstitution on *in Vitro* Growth of Tumor. To determine whether PTEN exerts control over angiogenesis and the growth of glial tumors, we developed an orthotopic brain tumor model in which PTEN-deficient tumor cells were genetically manipulated in vitro and then stereotactically injected into the skin or frontal cerebral cortex of nude mice. The U87MG cell line is derived from a patient diagnosed with glioblastoma multiforme, a highly malignant and uniformly fatal brain tumor. This tumor and other human glioblastomas and glioblastoma cell lines contain a mutation in both PTEN alleles, resulting in a null genotype. In light of these observations, we reconstituted the PTEN gene in the parental U87MG (U87) cells.

Stable derivatives of the parental U87 cells were generated after transduction with retroviruses encoding cDNA for WT PTEN or specific mutants of this phosphatase. In particular, we used missense mutations in the PTP signature motif to ascertain the importance of the enzymatic activity of PTEN to its tumor suppressor function. This included R130 M, in which all phosphatase activity is abrogated (5, 33), and G129E, which has been identified in Cowden disease and endometrial cancer and in which the activity toward inositol phospholipids is severely attenuated but protein phosphatase activity is essentially intact.

Tumor cells were characterized biochemically for levels of activated AKT (phospho-S473-AKT), growth *in vitro*, and PTEN expression (Fig. 1). Anti-PTEN blots confirmed that parental

U87 cells do not express PTEN and that after reconstitution of mutant or WT PTEN expression, U87 cells express amounts comparable to WT physiological levels. Expression of WT PTEN, to levels similar to those observed in a mouse brain lysate and primary human astrocytes, suppressed the activated state of AKT observed in PTEN-deficient U87 cells (Fig. 1*A*, lanes 3 and 5). After expression of the R130 M and G129E mutant forms of PTEN, the levels of phospho-AKT were similar to those observed in the parental U87 cells (Fig. 1*A*, lanes 1, 2, and 4), suggesting that the lipid phosphatase activity of PTEN was essential for the effects on the PtdIns(3,4,5)P$_3$-dependent activation of AKT. Importantly, the growth of the different PTEN-expressing U87 cell lines *in vitro* was similar in 2%, 5%, and 10% FBS (data not shown and Fig. 1*B*). Therefore, we compared these cell lines further in our *in vivo* models.

Effect of PTEN Reconstitution on *in Vivo* Growth and Proliferation. We implanted athymic nude mice s.c. and by intracranial injection. Production of s.c. tumors allowed us to monitor the size of the tumor and perform direct biochemical analysis of tumor tissue for PTEN expression and levels of AKT activation without significant contamination from other tissues. Tumor tissue blocks were processed for hematoxylin/eosin staining. Greater than 95% of tissue analyzed was tumor. We compared the levels of PTEN in tumor tissue and numerous normal tissues within the athymic nude mouse. Using anti-PTEN antisera, we detected the expression of PTEN in all tissues, with the exception of skeletal and heart muscle (data not shown), but no PTEN was detected in parental U87-derived tumor tissue (Fig. 2*C*, lane 4). These results indicate that the tumor tissue sampled represents predominantly tumor cell-derived proteins. As observed in the cell lines grown *in vitro*, s.c. tumors, derived from U87 cells reconstituted with mutant or WT PTEN, displayed similar levels of PTEN expression (Fig. 2*C*, lanes 1–3 and 5). Phospho-AKT activity was higher in PTEN-null U87 cells and U87 cells reconstituted with R130 M and to a lesser extent in U87 cells expressing the G129E mutant (Fig. 2*C*, lane 1) as compared with the WT PTEN-transduced cells (Fig. 2*C*, compare lanes 1, 2, and 4 to lanes 3 and 5). The pattern of phosphorylated AKT was similar when the different U87 mutant expressing cell lines were assayed *in vitro* or *in vivo* (compare Fig. 1*A* to 2*C*).

Despite the similar *in vitro* growth rate, there was a dramatic difference in the growth of tumors derived from parental U87 cells compared with cells reconstituted with WT PTEN (Fig. 2*A* and *B*). The average volume of U87-derived tumors on day 25 after implantation was 848 ± 203 mm^3, compared with 91 ± 27 mm^3 for tumors derived from WT PTEN-reconstituted cells ($n = 5$, $P < 0.0001$). Interestingly, the reconstitution of U87 cells with catalytically impaired PTEN (G129E or R130 M mutants) (Fig. 2*A*) shows an intermediate level of growth suppression, a result that suggests some residual function of these mutants *in vivo*.

Despite dramatic differences in the size of these tumors, *in vivo* BrdUrd labeling of tumor cells revealed no significant difference in number of cells in S phase: 72 ± 6 BrdUrd-positive cells per field in parental U87MG tumor mass versus 68.5 ± 3 in WT PTEN reconstituted tumors (data not shown). The percentage of TUNEL-positive nuclei within the U87MG and WT PTEN reconstituted tumors was similar. These results suggested that something other than the proliferative or apoptotic rate of the U87MG versus U87MG reconstituted with WT PTEN accounted for the difference in growth potential. We observed that the loss of inositol phospholipid phosphatase activity results in deregulated tumor growth comparable to the total ablation of catalytic activity and that the despite differences in overall growth *in vivo*, the proliferative rate of these tumors is similar. These findings are consistent with a role for PTEN in the regulation of another aspect of tumor biology, such as angio-
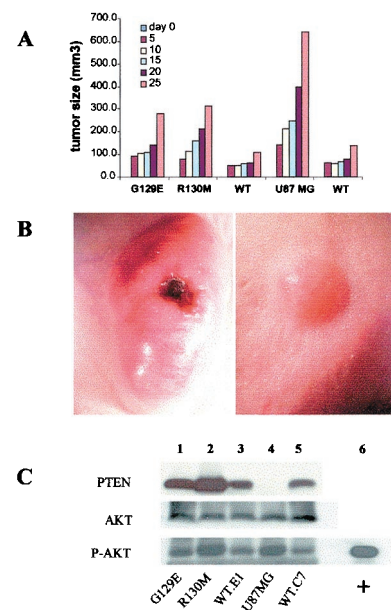

Fig. 2. Effects of PTEN on growth of U87MG cells *in vivo*. (*A*) Cell growth *in vivo*. To determine the rate of cell growth *in vivo*, equal amounts of cells (5 × 10^6) from each cell line were implanted at the right ventral flank by s.c. injection. The formation and growth of the s.c. tumor was monitored, and the volume of the tumor was determined by a three-dimensional measurement at the times indicated (day 0, the date of implantation, no tumor is detected). Data were analyzed by Student's *t* test, and differences were significant comparing the PTEN deficient (U87MG, R130 M, G129E) to the WT PTEN (WT.E1, WT.C7), $n = 5$, number of mice; $P < 0.0001$. (*B*) Stereophotography of s.c. tumor sites in mice implanted with the parental U87 tumor, PTEN minus (*Left*) versus WT PTEN reconstituted tumor cells (*Right*). These tumors represent 25 and 42 days after implantation for PTEN minus versus WT PTEN reconstituted tumors, respectively. (Magnification, ×40.) (*C*) Immunoblot of cryostat tissue sections from s.c. tumor for the expression pattern of PTEN, AKT, and phosphorylated AKT. Frozen tissue sections were solubilized in Laemmli sample buffer, total protein was quantitated, and equal protein was loaded on SDS/PAGE. The data shown are representative of tissue analysis from five animals per experimental group.

genesis. This led us to assess the effect of PTEN reconstitution on the induction of angiogenesis in this model.

PTEN Suppresses Tumor-Induced Angiogenesis. To examine the effect of PTEN on angiogenesis, we compared parental U87 cells to cells reconstituted with WT or mutant PTEN. We stained cryostat sections from s.c. tumors for CD31 (PECAM). CD31 is an endothelial marker used to measure the MVD of these tumors. MVD was assessed from multiple digitized images of CD31-stained tumor tissue at ×100 magnification (three fields were evaluated per tumor) and counted blindly for the number of CD31-positive microvessels per unit surface area as described (32). Reconstitution of PTEN expression in U87 cells dramatically suppressed the angiogenic response *in vivo* (Fig. 3 *A* and *B*). Quantitation of MVD in tumors derived from parental U87 cells (77 ± 13) and U87 cells expressing WT PTEN (38 ± 7) revealed an ≈50% suppression of angiogenesis (Fig. 3*C*) ($n = 5$, $P < 0.001$). The MVD of tumors derived from U87 cells reconstituted with catalytically impaired PTEN (R130 M, 84 ± 15 or G129E, 69 ± 16) were not significantly different ($P > 0.05$) from the parental U87 cell line (Fig. 3*C*). The levels of phospho-AKT detected within the tumor mass *in vivo* provide a correlation between the loss of the inositol lipid phosphatase function of PTEN, the phosphorylation status AKT, and the angiogenic phenotype within the tumor.

PTEN Induction of Thrombospondin. Recent *in vitro* data suggest a link between PTEN and downstream targets including AKT,

DOCKET ALARM

Explore Litigation Insights

Docket Alarm provides insights to develop a more informed litigation strategy and the peace of mind of knowing you're on top of things.

Real-Time Litigation Alerts

Keep your litigation team up-to-date with **real-time alerts** and advanced team management tools built for the enterprise, all while greatly reducing PACER spend.

Our comprehensive service means we can handle Federal, State, and Administrative courts across the country.

Advanced Docket Research

With over 230 million records, Docket Alarm's cloud-native docket research platform finds what other services can't. Coverage includes Federal, State, plus PTAB, TTAB, ITC and NLRB decisions, all in one place.

Identify arguments that have been successful in the past with full text, pinpoint searching. Link to case law cited within any court document via Fastcase.

Analytics At Your Fingertips

Learn what happened the last time a particular judge, opposing counsel or company faced cases similar to yours.

Advanced out-of-the-box PTAB and TTAB analytics are always at your fingertips.

API

Docket Alarm offers a powerful API (application programming interface) to developers that want to integrate case filings into their apps.

LAW FIRMS
Build custom dashboards for your attorneys and clients with live data direct from the court.

Automate many repetitive legal tasks like conflict checks, document management, and marketing.

FINANCIAL INSTITUTIONS
Litigation and bankruptcy checks for companies and debtors.

E-DISCOVERY AND LEGAL VENDORS
Sync your system to PACER to automate legal marketing.